Water Stable Perovskite Nanocrystal for Highly Efficient Photoinduced RAFT Dispersion Polymerization

Runqian Zhang[1‡], Wenjie Zhang[1‡], Chengli Wang[1], Xiaomeng Zhang[1], Zhe Cui[1], Peng Fu[1], Minying Liu[1], Yajing Chang[2], Zhibin Zhang[3], Yanjie He[1], Xinchang Pang[1,3*]*

1. Henan Joint International Research Laboratory of Living Polymerizations and Functional Nanomaterials, Henan Key Laboratory of Advanced Nylon Materials and Application, School of Materials Science and Engineering, Zhengzhou University, Zhengzhou, 450001, P. R. China.

2. State Key Laboratory of Pulsed Power Laser Technology, National University of Defense Technology, Hefei, Anhui, 230037, P. R. China.

3. School of Materials Science and Engineering, Henan University of Science and Technology, Luoyang 471023, P. R. China.

Corresponding Author

he_yanjie@zzu.edu.cn; Pangxinchang1980@163.com

Chemicals

Lead (II) bromide ($PbBr_2$, 99.999%), cesium bromide (CsBr, 99.9%), cesium carbonate (Cs_2CO_3, 99.9%), oleic acid (OA, 90%), oleylamine (OAm, 70%), 1-octadecene (ODE, 90%), 5-bromovaleric acid (BVA, 97%), 4-bromobutyric acid (BBA, 98%), sodium dodecyl sulfate (SDS, 98.5%), sodium lauryl sulfate (SLS, 98%), polyvinyl alcohol (PVA, 98%, 5.2-6.0 mPa.s), and polyethylene glycol (PEG, 8000 g/mol), N-dimethylacetamide (DMA, 99.9%), toluene (TL, 99.5%), methyl acetate (MeOAc, 99%), monomethoxy poly (ethylene glycol) (mPEG, 5000 g/mol), monomethoxy poly (ethylene glycol) (mPEG, 1900 g/mol), 4-dimethylaminopyridine (99%), 1-(3-dimethylaminopropyl)-3-ethylcarbodiimide (hydrochloride) (EDC·HCl, 99.8%), dichloromethane (99.5%), diethyl ether (99%), 1-butanethiol (97%), carbon disulfide (99.5%), 2-bromopropionic acid (98%), n-hexane (97%), acetone (99.5%), ethanol (99.8%), tetrabutylammonium hexafluorophosphate ($TBAPF_6$, 98%) and sodium hydroxide (97%) were purchased from Sigma Aldrich and used without any further purification. Methyl methacrylate (MMA, 99%, stabilized with 30 ppm DMBP), 2-hydroxyethyl acrylate (HEA, 99%,stabilized with 200-600 ppm MEHQ), 2,2,2-trifluoroethyl methacrylate (TFEMA, 98%, stabilized with 100 ppm MEHQ), 3, 3, 4, 4, 5, 5, 6, 6, 7, 7, 8, 8, 9, 9, 10, 10, 10-heptadecafluorodecyl methacrylate (HDFDMA, 98%), styrene (St, 99%, stabilized with 10-15ppm TBC) and butyl methacrylate (BMA, 99%, stabilized with MEHQ) were distilled in the presence of calcium hydride under reduced pressure to remove inhibitors prior to aqueous dispersion polymerization.

Synthesis of Water-Stable Oleylamine/Bromovaleric Acid Capped $CsPbBr_3$

Nanocrystals (denoted as OAm/BVA-$CsPbBr_3$ NCs)

A mixture of 0.2 mmol $PbBr_2$ (73.4 mg) and 0.2 mmol CsBr (42 mg) was introduced into a 25 mL reaction flask containing 5 mL of DMA solution. The mixture was heated to 50 °C and magnetically stirred for 1 h to obtain a clear solution. Subsequently, 1 mmol of OAm was introduced, and vigorous stirring was continued for an additional 20 min. Afterward, 1 mmol of BVA was added to the solution, followed by another 20 min of stirring, resulting in a yellow cloudy solution (denoted as Solution A). Then, 2 mL of Solution A was rapidly injected into 12 mL of 50 °C water within 5 s under vigorous stirring at the desired temperature. After the injection, the reaction mixture was immediately quenched in an ice bath and magnetically stirred for another 5 min. For purification, 5 mL of the stock solution was centrifuged at 3000 rpm for 3 min, and the yellow precipitate solid in the bottom of the centrifugal tube was discarded. The supernatant was centrifuged at 10000 rpm for 25 min, the precipitate was re-dispersed in 5 mL of deionized water and stored at 5 °C in the dark for characterizations as well as for further usage in subsequent aqueous photopolymerization.

Synthesis of Conventional Oleylamine/Oleic Acid Capped $CsPbBr_3$ Nanocrystals (denoted as OAm/OA-$CsPbBr_3$ NCs)

The preparation of OAm/OA-$CsPbBr_3$ NCs was followed by classic work reported by Kovalenko's group.[1] Generally, Cs_2CO_3 (0.814 g) was mixed with octadecene (40 mL, ODE) and oleic acid (2.5 mL) in a 100 mL three-neck flask. The mixture was dehydrated at 120 °C for 1 h under nitrogen flow, followed by heating to 150 °C until complete reaction

of the cesium precursor with oleic acid was achieved (0.125 M in ODE). Due to the precipitation of Cs-oleate in octadecene at room temperature, the precursor solution required preheating to100°C prior to the hot-injection reaction.

In a typical synthesis experiment of perovskite nanocrystal, ODE (5 mL) and $PbBr_2$ (69 mg) were introduced into a 25 mL three-necked flask, where they were dried under vacuum at 120 °C for 1 h. Afterward, pre-dried OAm (0.5 mL) and dried OA (0.5 mL) were swiftly injected into the flask under a nitrogen atmosphere at 120 °C. Upon complete dissolution of the $PbBr_2$ precursor, the temperature was elevated to 150 °C, and a 0.4 mL solution was promptly injected. 5 s later, the reaction mixture was rapidly quenched using an ice-water bath. For purification, 2 mL of the stock solution was centrifuged at 10000 rpm for 15 min to get rid of large perovskite crystal. The supernatant was further purified by using methyl acetate as a precipitating solvent and toluene as a good solvent twice. The resulting purified precipitate was re-dispersed in 5 mL of toluene for subsequent characterizations and dispersion photopolymerization.

Synthesis of 2-(Butylsulfanyl)carbonothioyl Sulfanyl Propanoic Acid (BTPA) as Chain Transfer Agent

The synthesis process was followed by previously published work.[2] A 90 mL solution of sodium hydroxide (16.0 g, 0.40 mol, 4.4 M) was added dropwise to a mixture of 1-butanethiol (43.00 g, 0.47 mol) and 20 mL of acetone in a 500 mL three-necked flask and maintained at 15 °C using a water bath. The solution was stirred for 30 min, after which 30 mL of carbon disulfide was added dropwise, followed by an additional 30 min of stirring.

Subsequently, 2-bromopropionic acid (66.0 g, 0.43 mol) was introduced, followed by the addition of another 30 mL of sodium hydroxide solution (4.4 M) and 25 mL of deionized water. The mixture was then allowed to stir for 24 h at room temperature. The resulting orange mixture was extracted using 50 mL concentrated hydrochloric acid (12 M) at 0 °C and filtered to obtain a yellow solid. This raw product was repeatedly washed with cold water at 5 °C, dried in a vacuum chamber at 25 °C, and finally dissolved in 200 mL hexane at 60 °C. Recrystallization at 0 °C in hexane yielded 107.3 g (0.45 mol) of the product, which corresponded to a 95% yield. Proton nuclear magnetic resonance (^{1}H NMR) measurement revealed the presence of the following protons: δ = 3.45 (t, SCH_2C), 1.65 (m, CCH_2C), 1.45 (m, CCH_2'C, and 0.90 (t, CH_3C). ^{13}C NMR also showed the presence of the following carbon atoms: δ = 205.61 (s, SCSS), 36.23 (s, SCH_2C), 30.18 (m, CCH_2C), 29.84 (m, CCH_2'C, note: same as above, check for structural difference), 21.97 (q, C-methyl of the acid moiety, if applicable, otherwise adjust description), and 13.22 (s, CH_3C).

Synthesis of Methoxy Poly (ethylene glycol) (2-((butylsulfanyl) carbonothioyl) sulfanyl) Propanoate (denoted as mPEG-BTPA) Macro-RAFT Agent via Coupling Reaction

4.2 g mPEG (0.84 mmol, 5000 g mol^{-1}), 0.3 g BTPA (1.26 mmol), and 15.3 mg 4-dimethylaminopyridine (DMAP, 0.126 mmol) were dissolved in 10 mL dichloromethane at 25 °C to form a transparent solution. Subsequently, 0.241 g of 1-(3-dimethylaminopropyl)-3-ethylcarbodiimide hydrochloride (EDC·HCl) (1.26 mmol) was gradually added to the

solution at 0 °C. The mixture was then stirred for 48 h at 25 °C. The raw product was precipitated twice in cold diethyl ether and filtered. The filtrate was dried under vacuum at room temperature. For further purification, The dried product was redissolved in deionized water (60 mL) and dialyzed against deionized water using a dialysis membrane (MWCO 1000 Da) for 3 days. After dialysis, the product was lyophilized, yielding a light-yellow powder-like product.

Photo-induced Aqueous Reversible Addition–Fragmentation Chain Transfer (RAFT) Polymerization Catalyzed by OAm/BVA-$CsPbBr_3$ Nanocrystal [3]

To demonstrate the structural robustness of OAm/BVA-$CsPbBr_3$ NC and its potential application in aqueous photopolymerization, this water-stable perovskite nanocrystal was utilized as a photocatalyst in the homogeneous aqueous photo-induced RAFT polymerization of 2-hydroxyethyl acrylate (HEA). In a 5 mL Schlenk flask, 1 mL of OAm/BVA-capped $CsPbBr_3$ NCs stock solution was added to a mixture consisting of 1 mL of HEA (9.56 mmol) and 5.69 mg of BTPA (0.0478 mmol) as a RAFT agent. The Schlenk flask was sealed with a septum and deoxygenated by a freeze-pump-thaw cycling process to remove dissolved oxygen in the reaction solution. Polymerization was then initiated under blue LED (λ_{max} = 460 nm) irradiation. The aliquots were withdrawn from the solution to monitor monomer conversion. As-synthesized poly (2-hydroxyethyl acrylate) was purified by dialysis in DI water for 3 days to remove excess monomer and impurities. The final product (i.e., poly (2-hydroxyethyl acrylate), PHEA) was obtained by lyophilization and used for subsequent characterizations.

Synthesis of Uniform PMMA Microspheres by Photoinduced Aqueous RAFT Dispersion Polymerization

In a typical experiment of photoinduced aqueous RAFT dispersion polymerization, 0.25 g MMA (2.5 mmol), 18 mg $mPEG_{5K}$-BTPA (0.0034 mmol) as a macro-RAFT agent, and 0.03 mg BTPA as a co-RAFT agent (0.0001 mmol) were dissolved in 1.14 mL of ethanol (0.9 g) in a 10 mL Schlenk flask at 30 °C. Subsequently, 1.35 mL of OAm/BVA-capped $CsPbBr_3$ NCs stock aqueous solution was rapidly added to the mixture. The mixed solution was deoxygenated by a freeze-pump-thaw cycling process to remove dissolved oxygen in the reaction solution, backfilled with N_2, and then irradiated under blue LED lamp (λ_{max} = 460 nm, 42 W/cm^2) for a certain period of time. The reaction mixture gradually changed from a clear transparent to a cloudy solution. The resulting milky solution was purified by centrifugation and repeatedly rinsed with an ethanol/water mixture (40/60, w/w). After washing, the microspheres were dried in a vacuum oven for 24 h to obtain a fine white powder, which was then weighed to determine the monomer conversion yield. The resulting purified polymer microspheres could be easily dispersed in water to obtain a stable colloidal solution for transmission electron microscope analysis and other characterizations.

To demonstrate the versatility of our approach, this photoinduced aqueous RAFT dispersion polymerization was extended to other monomers by replacing the MMA with other vinyl monomers with other polymerization conditions fixed. The purification of as-synthesized polymer microspheres was analogous to the above-mentioned procedure.

In addition, the blue LED light source was switched to a near-infrared laser to perform near-infrared (λ = 808 nm) light-induced aqueous RAFT dispersion polymerization of MMA with other conditions fixed. In a typical synthesis, 0.25 g (2.5 mmol) MMA, 18 mg (0.0034 mmol) $mPEG_{5K}$-BTPA, and 0.03 mg (0.0001 mmol) BTPA were dissolved in 1.14 mL ethanol in a 10 mL Schlenk flask. Then, 1.35 mL of OAm/BVA-capped $CsPbBr_3$ NCs aqueous solution was added. The mixture was deoxygenated via freeze-pump-thaw cycles, purged with N_2, and irradiated under near-infrared laser (λ = 808 nm,100 mW/cm^2) for 90 min. The resulting milky solution was purified by centrifugation and repeatedly rinsed with an ethanol/water mixture (40/60, w/w). After washing, the microspheres were dried in a vacuum oven for 24 h to obtain a fine white powder, which was then weighed to determine the monomer conversion yield. The resulting purified polymer microspheres could be easily dispersed in water to obtain a stable colloidal solution for subsequent characterizations.

Characterizations

The morphology of perovskite nanocrystals was investigated using transmission electron microscopy (TEM, JEOL 2100F) operated at 200 kV with a thermionic electron source. For TEM imaging, purified $CsPbBr_3$ nanocrystals or polymer microspheres were dispersed in DI water, drop-casted onto carbon-coated copper grids, and vacuum-dried overnight at room temperature. High-resolution TEM (HR-TEM) was performed to analyze crystallographic details. Scanning electron microscopy (SEM) was conducted using a JEM-F200 instrument at 15 kV accelerating voltage. Samples were deposited on clean silicon substrates from aqueous dispersions and sputter-coated with gold prior to imaging. X-ray

photo electron spectroscopy (XPS, Theme ScientificK-Alpha+, hv=1486.6 eV) was used to investigate the valence band and binding energies of the samples. Ultraviolet and visible absorption: (UV-vis) spectra were recorded on a Carry 5000-UV-vis spectrophotometer. Photoluminescence spectra were obtained by a fluorescence spectrofluorometer (LF-1802003), using 365 nm light as the excitation source. Fourier-transform infrared spectroscopy (FTIR, Themo Nicoletica 5) was used to identify functional groups in the 4000–500 cm^{-1} range. Crystalline phase identification was performed by powder X-ray diffraction (XRD, SMART LAB) using Cu-Kα radiation (λ = 0.154 nm, 40 kV). Samples were prepared by drop-casting $CsPbBr_3$ NCs onto quartz substrates followed by 2 h vacuum drying at room temperature. Phase identification was made using standard JCPDs files. The molecular weight and polydispersity of polymeric microspheres were determined by gel permeation chromatography (GPC, Waters 1515) using THF eluent (1 mL/min flow rate) with polystyrene standards for calibration. The residual lead content in the polymeric microsphere is determined by inductively coupled plasma mass spectrometry (ICP-MS). ^1H NMR spectra (400 MHz, Bruker Avance) were acquired in $CDCl_3$ at 25 °C to verify polymer chemical compositions and organic ligand coordination on the surface of perovskite nanocrystals. Photocurrent measurements were conducted under 365 nm UV illumination (5 mW cm^{-2}), with a scan rate of 100 mV s^{-1} and light on-off cycles of 10-second intervals. Gel permeation chromatography (GPC) analysis was performed using an Agilent 1260 Infinity ll system equipped with two PL gel 10 MIXED-B 300 x 7.5 mm columns, a column temperature of 45 °C, an RI detector and N, N-dimethylformamide (DMF) with 18 mM LiBr as an eluent at a flow rate of 1 mL/min. The system was calbrated with narrow-

dispersity polystyrene standards to determine the number-average molecular weight and dispersity (*Đ*) of mPEG. Electrochemical impedance spectroscopy (EIS) characterization was performed at a bias potential of -0.78 V under dark conditions. Transient photocurrent response was performed using a CHI660E electrochemical workstation with a standard three-electrode configuration. The system consisted of a platinum counter electrode and an Ag/AgCl reference electrode, with 10 M tetrabutylammonium hexafluorophosphate ($TBAPF_6$) solution serving as the electrolyte. For sample preparation, purified $CsPbBr_3$ NCs (1 mL) were mixed with Nafion (0.2 μL) under 1-minute ultrasonication, followed by spin-coating onto ITO glass substrates and drying in a vacuum oven at room temperature. Photocurrent measurements were conducted under 365 nm UV illumination (5 mW cm^{-2}), with a scan rate of 100 mV s^{-1} and light on-off cycles of 10-second intervals. EIS characterization was performed at a bias potential of -0.78 V under dark conditions.

Table S1. OAm/BVA-capped $CsPbBr_3$ NC-catalyzed photo-mediated homogenous RAFT polymerization of 2-hydroxyethyl acrylate (HEA) in water.

Entry	Catalyst	Monomer	DP	CTA	Time (min)	α (%)[e]	$M_{n,theo}$ (kg/mol) [f]	$M_{n,GPC}$ (kg/mol) [g]	M_w/M_n[h]
1	OAm/BVA-capped $CsPbBr_3$ NC	HEA	200	-	30	-	-	-	-
2	No	HEA	200	BTPA	30	-	-	-	-
3[a]	OAm/BVA-capped $CsPbBr_3$ NC	HEA	200	BTPA	30	-	-	-	-
4[b]	OAm/BVA-capped $CsPbBr_3$ NC	HEA	200	BTPA	30	-	-	-	-
5[c]	OAm/BVA-capped $CsPbBr_3$ NC	HEA	200	BTPA	30	-	-	-	-
6	OAm/BVA-capped $CsPbBr_3$ NC	HEA	200	BTPA	30	36.0	8.6	9.3	1.14
7[d]	OAm/OA-capped $CsPbBr_3$ NC	HEA	200	BTPA	30	-	-	-	-

Note: The dash symbol (-) indicates no monomer conversion.

a The homogenous aqueous photoinduced RAFT polymerization of HEA is conducted without deoxygenation process prior to blue light irradiation with other reaction conditions fixed.

b The homogenous aqueous photoinduced RAFT polymerization of HEA is conducted without blue light irradiation with other reaction conditions fixed.

c The homogenous aqueous photoinduced RAFT polymerization of HEA is conducted under green light irradiation with other reaction conditions fixed.

d The homogenous aqueous photoinduced RAFT polymerization of HEA is conducted using conventional OAm/OA-capped $CsPbBr_3$ NC as photocatalyst with other reaction conditions fixed.

e The monomer conversion is calculated by proton nuclear magnetic resonance spectra of reaction solution right after photopolymerization.

f The theoretical molecular weight of as-syntheiszed polymer is calculated using the

following equation: $M_{n,theo} = M_{w,RAFT\ agent}$ + Monomer Conversion*200*$M_{w,HEA}$

g The molecular weight of PHEA is measured by gel permeation chromatography using dimethylformamide as eluent.

h The molecular weight distribution (i.e., M_w/M_n) is calculated using M_w and M_n measured from gel permeation chromatography.

Table S2. OAm/BVA-capped $CsPbBr_3$ NC-catalyzed photo-mediated heterogeneous RAFT dispersion polymerization of MMA in water/ethanol mixed solution.

Entry	Catalyst	Monomer	CTA	Time (min)	Particle size (nm)[f]	$M_{n,GPC}$ (kg/mol)[g]
1	OAm/BVA-capped $CsPbBr_3$ NC	MMA	-	90	-	-
2	No	MMA	mPEG-BTPA	90	-	-
3[a]	OAm/BVA-capped $CsPbBr_3$ NC	MMA	mPEG-BTPA	90	-	-
4[b]	OAm/BVA-capped $CsPbBr_3$ NC	MMA	mPEG-BTPA	90	-	-
5[c]	OAm/BVA-capped $CsPbBr_3$ NC	MMA	mPEG-BTPA	90	-	-
6	OAm/BVA-capped $CsPbBr_3$ NC	MMA	mPEG-BTPA	90	630 ± 21	68.3
7[d]	OAm/OA-capped $CsPbBr_3$ NC	MMA	mPEG-BTPA	90	-	-
8[e]	OAm/BVA-capped $CsPbBr_3$ NC	MMA	mPEG-BTPA	90	588 ± 84	55.0

Note: The dash symbol (-) indicates the absence of polymerization microparticles.

a The heterogeneous photoinduced RAFT dispersion polymerization of MMA is conducted without deoxygenation process prior to blue light irradiation with other conditions fixed.

b The heterogeneous photoinduced RAFT dispersion polymerization of MMA is conducted without blue light irradiation with other conditions fixed.

c The heterogeneous photoinduced RAFT dispersion polymerization of MMA is conducted under green light irradiation with other conditions fixed.

d The heterogeneous photoinduced RAFT dispersion polymerization of MMA is conducted using conventional OAm/OA-capped $CsPbBr_3$ NC as photocatalyst with other conditions fixed.

e The heterogeneous photoinduced RAFT dispersion polymerization of MMA is conducted under 808 nm near-infrared light irradiation.

f The size of polymer microparticles is determined from corresponding TEM images.

g The molecular weight of polymer microparticles is measured by gel permeation chromatography using dimethylformamide as eluent.

Table S3. Photo-mediated heterogeneous RAFT dispersion polymerization of MMA in water/ethanol mixed solution using $CsPbBr_3$ NC synthesized with different ligands.

Entry	Catalyst[a]	Monomer	CTA	Time (min)	Particle size (nm)[b]	$M_{n,GPC}$ (kg/mol)[c]
1	OAm/BVA-capped $CsPbBr_3$ NC	MMA	mPEG-BTPA	90	630 ± 21	68.3
2	OAm/BBA-capped $CsPbBr_3$ NC	MMA	mPEG-BTPA	90	512 ± 67	45.9
3	OAm/SDS-capped $CsPbBr_3$ NC	MMA	mPEG-BTPA	90	-	-
4	OAm/SLS-capped $CsPbBr_3$ NC	MMA	mPEG-BTPA	90	-	-
5	OAm/PVA-capped $CsPbBr_3$ NC	MMA	mPEG-BTPA	90	-	-
6	OAm/PEG-capped $CsPbBr_3$ NC	MMA	mPEG-BTPA	90	-	-

Note: The dash symbol (-) indicates the absence of polymerization microparticles.

a $CsPbBr_3$ NC with different ligands were synthesized by replacing BVA with equimolar amounts of other ligands with other conditions fixed.

b The size of polymer microparticles is determined from corresponding TEM images.

c The molecular weight of polymer microparticles is measured by gel permeation chromatography using dimethylformamide as eluent.

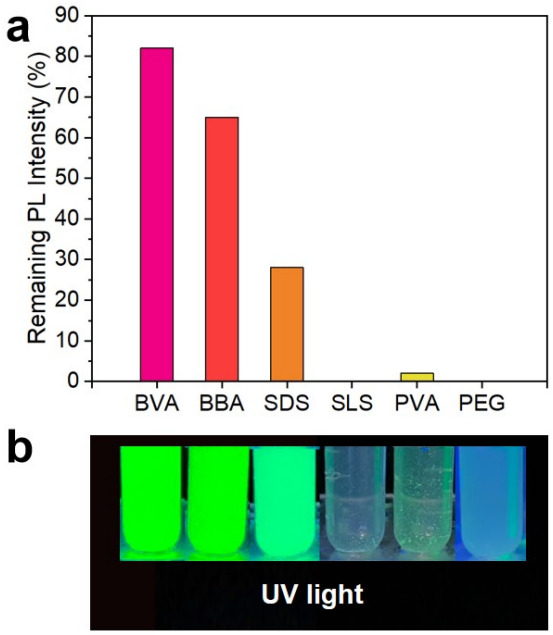

Figure S1. Stability tests of $CsPbBr_3$ NCs synthesized using amphiphilic ligands: 5-bromovaleric acid (BVA), 4-bromobutyric acid (BBA), sodium dodecyl sulfate (SDS), sodium lauryl sulfate (SLS), polyvinyl alcohol (PVA), and polyethylene glycol (PEG). (a) Retention rate of the photoluminescence intensity for $CsPbBr_3$ NCs modified with different ligands after 30 days of storage at room temperature. (b) Digital photographs of the $CsPbBr_3$ NC solutions with different ligands under ultraviolet light after 30 days of storage.

Note: 5-bromovaleric acid (BVA) demonstrates superior water stability for perovskite nanocrystals compared to conventional ligands-capped (e.g., BBA, SDS, SLS, PVA, and PEG) nanocrystals due to its unique dual-functional coordination mechanism. The carboxyl group (-COOH) forms strong bidentate chelates with undercoordinated Pb^{2+} sites, while the terminal bromine (-Br) simultaneously passivates halogen vacancies, creating a a protective stabilization that resists water diffusion. In contrast, ionic surfactants (i.e., SDS

or SLS) rely on weaker electrostatic adsorption that competes unfavorably with water molecules. For the case of perovskite nanocrystals prepared via polymeric ligands (i.e., PVA or PEG), the instability issue is primarily originated form the fact that both polymers have high tendency to dissolve in aqueous solution. The capped polymer ligands would be easily stripped from the surface of perovskite nanocrystals, resulting exposure of surface atoms of perovskite nanocrystals to water molecules. As a result, the perovskite nanocrystals could be rapidly decomposed.

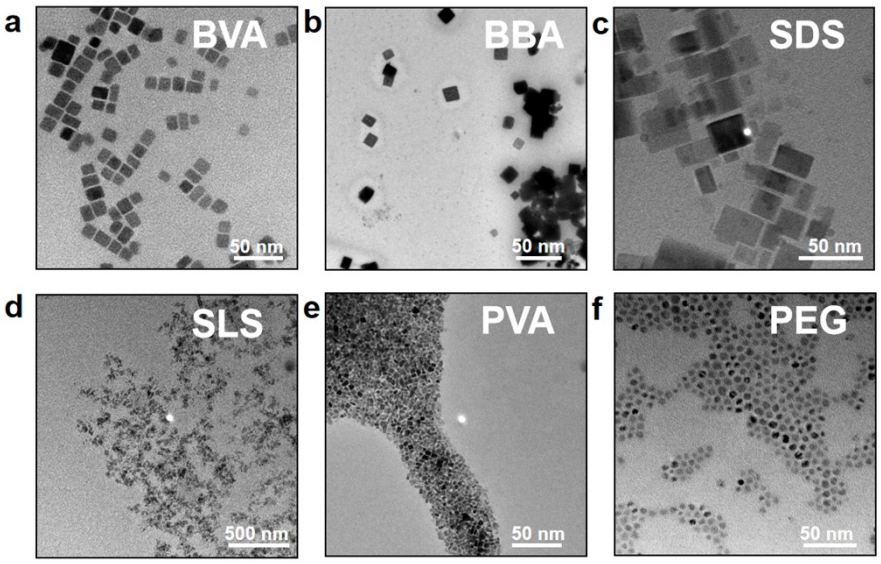

Figure S2. Transmission electron microscopy (TEM) images of $CsPbBr_3$ nanocrystals prepared using amphiphilic ligands.

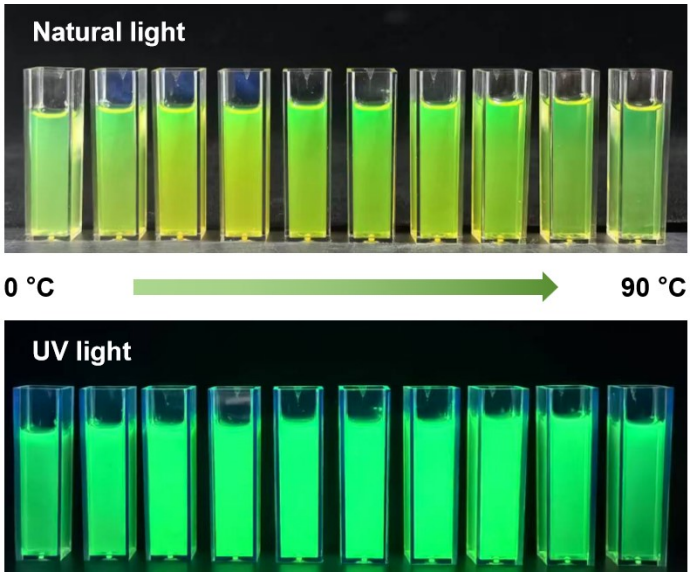

Figure S3. Digital images of OAm/BVA-capped $CsPbBr_3$ NCs aqueous solution synthesized at distinct reaction temperature under natural light and 365 nm UV light excitation.

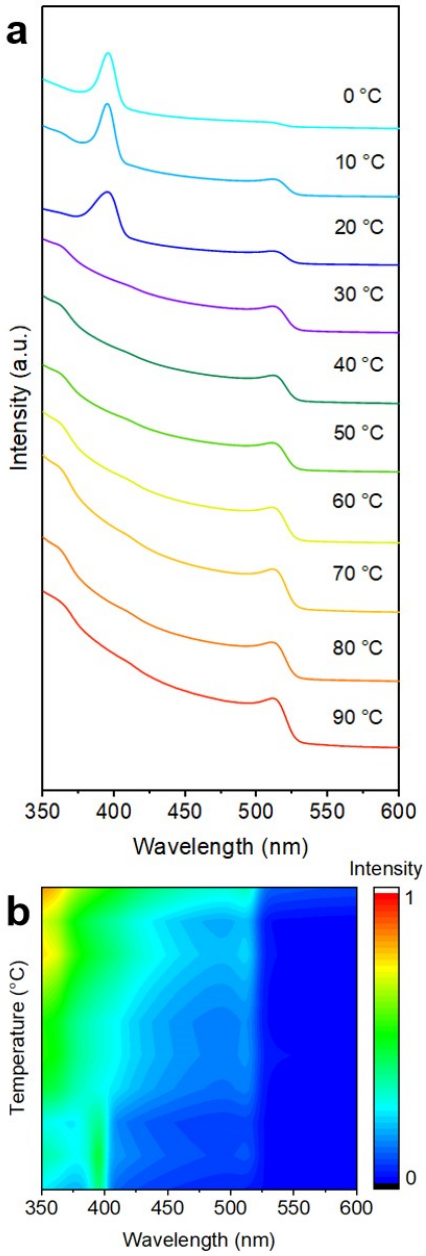

Figure S4. (a,b) Ultraviolet−visible (UV-Vis) absorption spectra of OAm/BVA-capped $CsPbBr_3$ NCs synthesized at distinct reaction temperature.

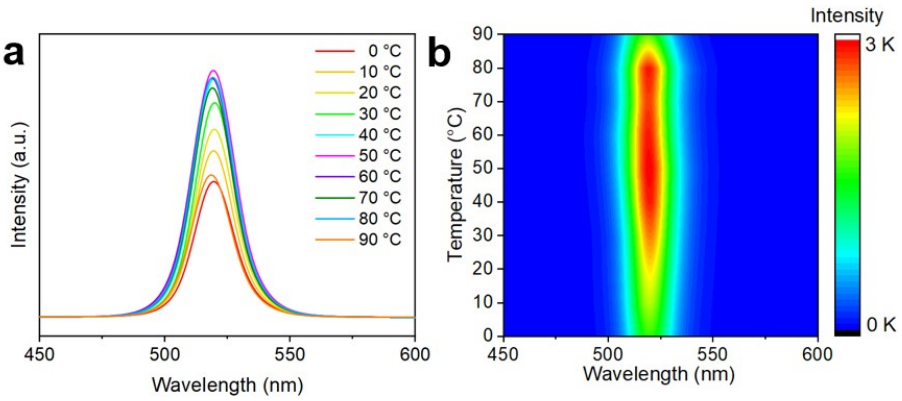

Figure S5. (a,b) Photoluminescence (PL) spectra of water stable OAm/BVA-capped $CsPbBr_3$ NCs synthesized at distinct reaction temperature.

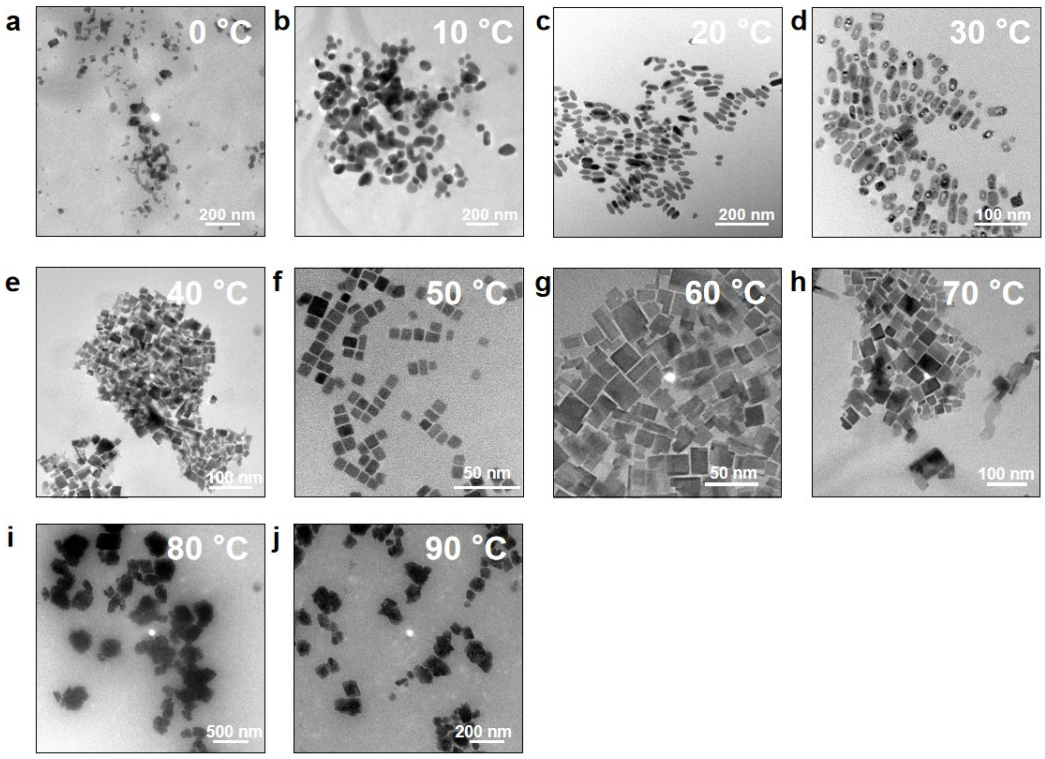

Figure S6. TEM images of water-stable OAm/BVA-capped $CsPbBr_3$ NCs synthesized at distinct reaction temperature.

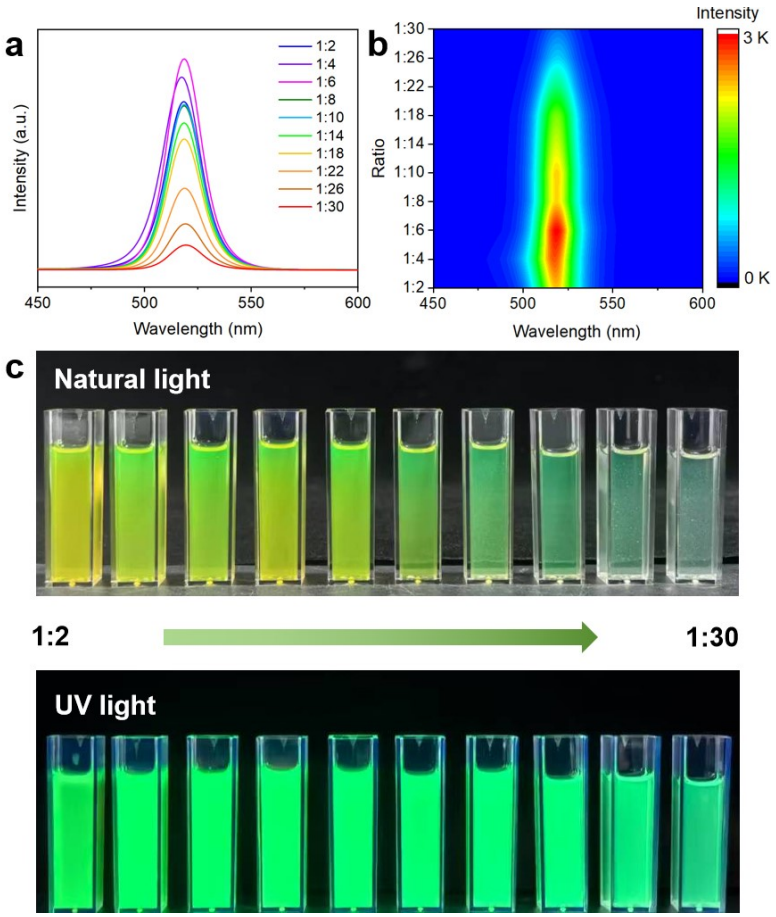

Figure S7. (a,b) PL spectra of OAm/BVA-capped $CsPbBr_3$ NCs prepared utilizing different volume ratios of precursor solution (the molar ratio of CsBr to $PbBr_2$ is maintained at 1:1) to DI water at 50 °C and (c) the corresponding digital images of OAm/BVA-capped $CsPbBr_3$ NCs aqueous solution under natural light and 365 nm UV light excitation.

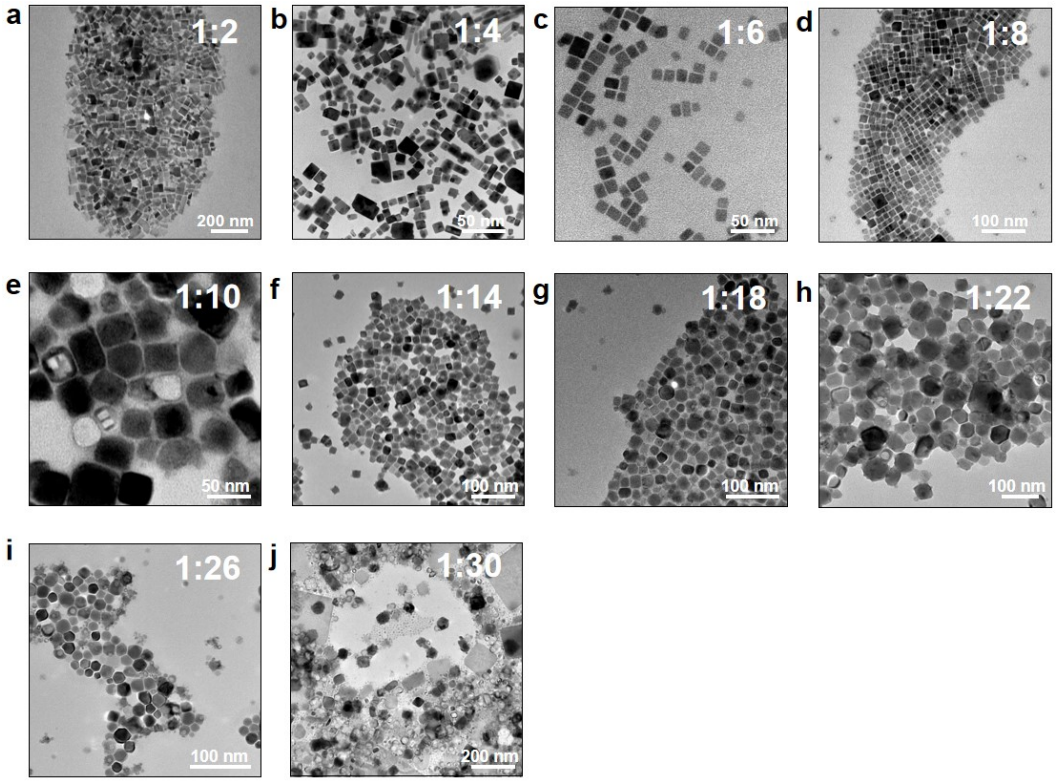

Figure S8. TEM images of OAm/BVA-capped $CsPbBr_3$ NCs prepared utilizing different volume ratios of precursor solution (the molar ratio of CsBr to $PbBr_2$ is maintained at 1:1) to DI water at 50 °C

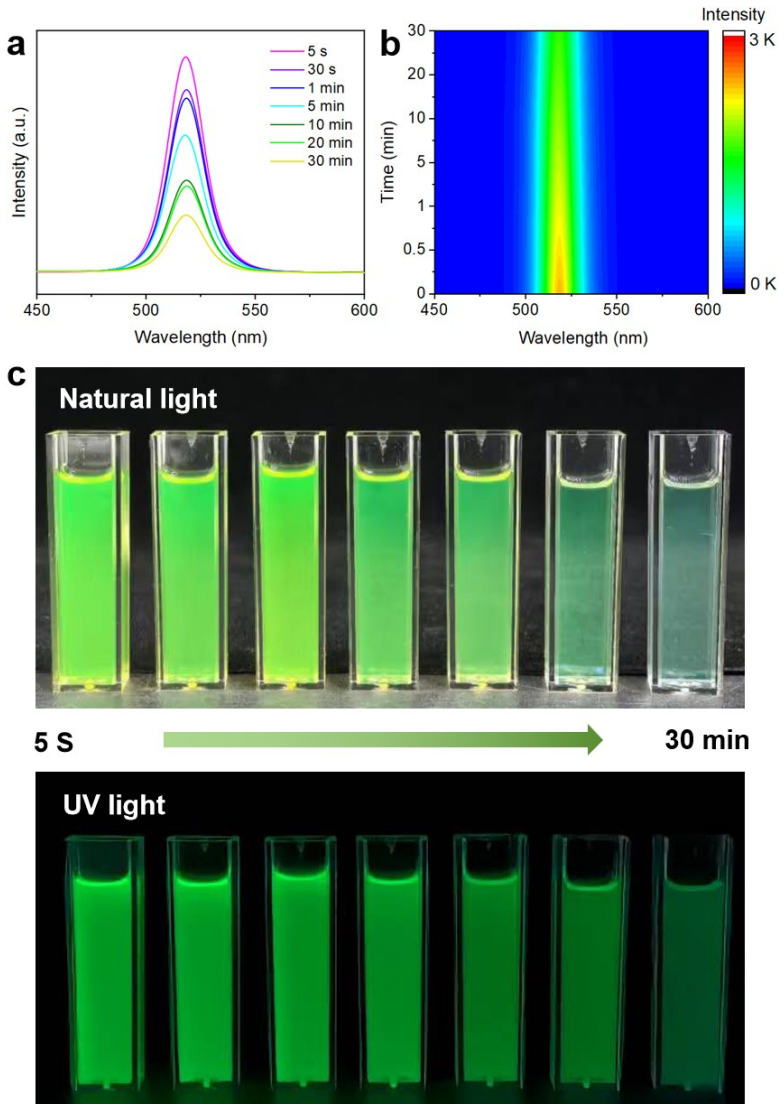

Figure S9. The effect of post-injection stirring time on the OAm/BVA-capped $CsPbBr_3$ NCs. (a,b) PL spectra and (c) digital images of aqueous OAm/BVA-capped $CsPbBr_3$ NCs colloidal solution. The injection temperature was maintained at 50 °C.

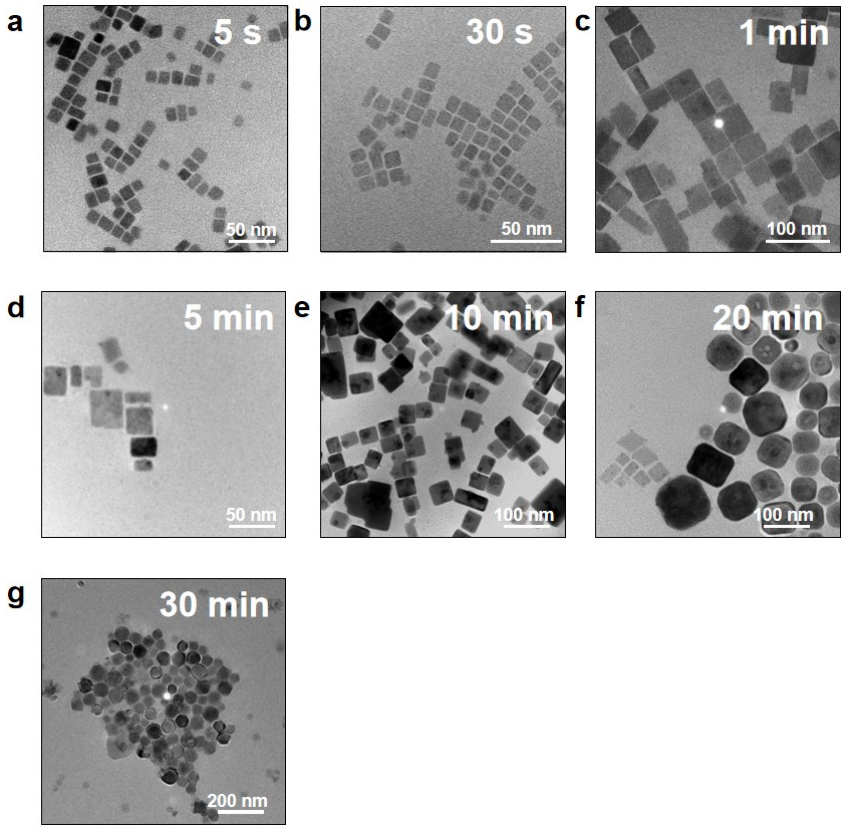

Figure S10. TEM images of OAm/BVA-$CsPbBr_3$ NCs with different post-injection stirring time. The injection temperature was maintained at 50 °C.

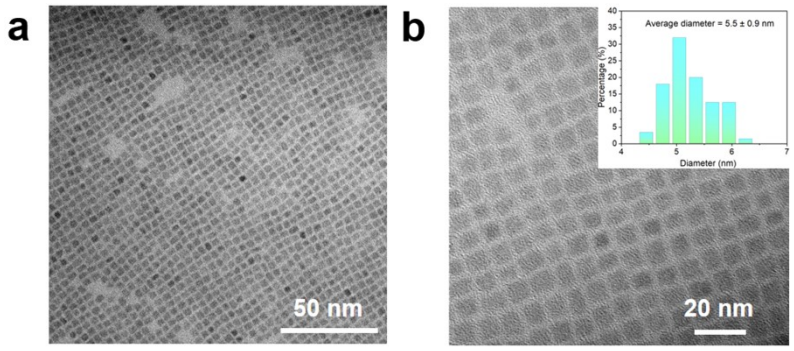

Figure S11. Transmission electron microscope (TEM) image and size distribution of traditional OAm/OA-capped $CsPbBr_3$ NCs.

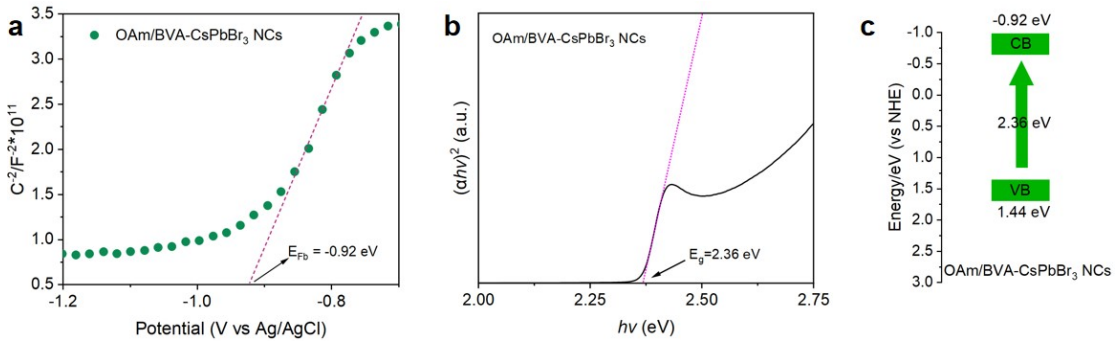

Figure S12. (a) Mott-Schottky plots, (b) Tauc plots, and (c) energy band structure diagram of OAm/BVA-$CsPbBr_3$ NCs.

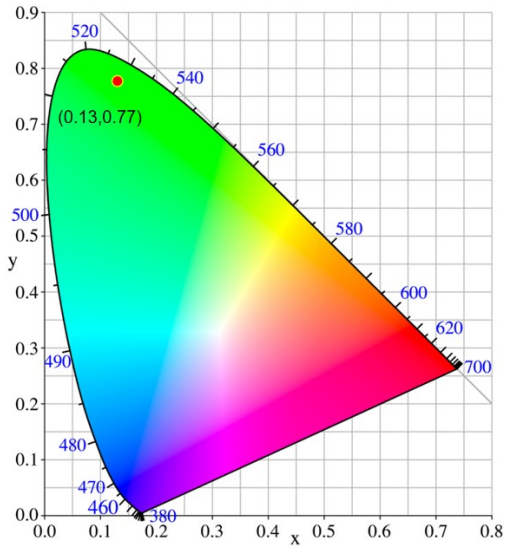

Figure S13. CIE color coordinate of water-stable OAm/BVA-capped $CsPbBr_3$ NCs

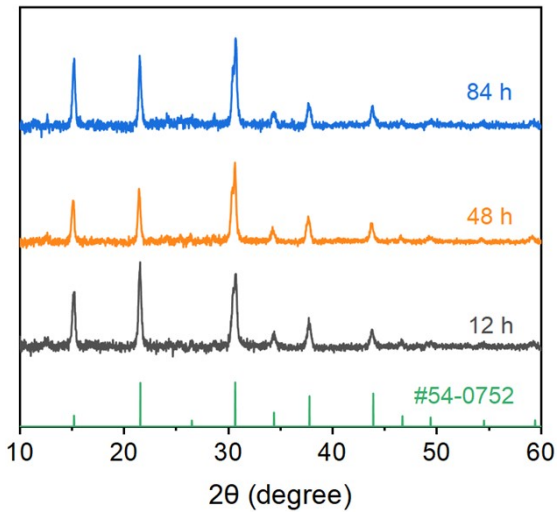

Figure S14. X-ray diffraction (XRD) patterns of OAm/BVA-capped $CsPbBr_3$ NCs stored in water for different periods of time.

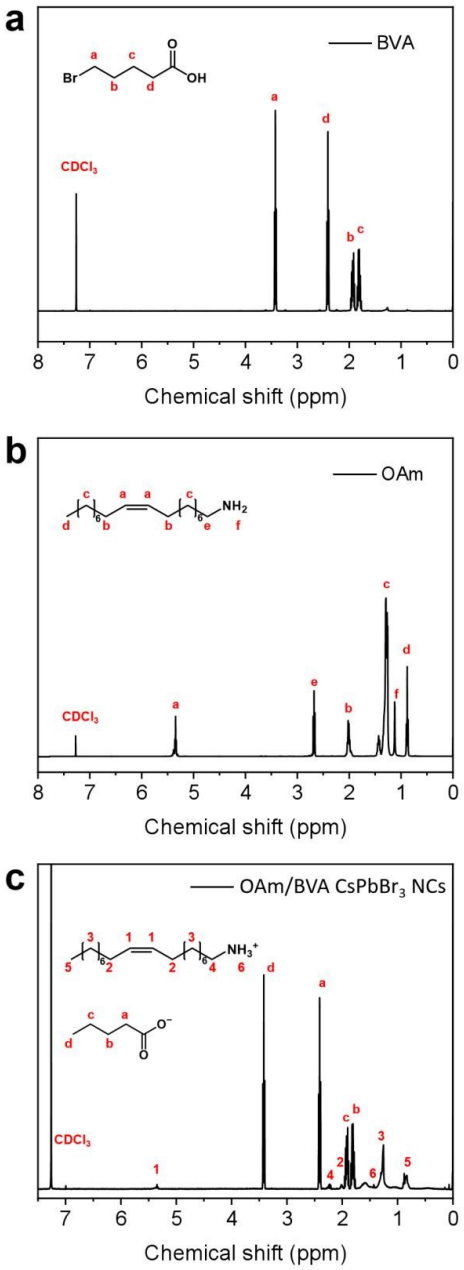

Figure S15. ^{1}H NMR spectra (in $CDCl_3$, at 298 K, with 500 MHz) of (a) pristine 5-bromovaleric acid (BVA), (b) pristine oleylamine (OAm) and (c) OAm/BVA-capped $CsPbBr_3$ NCs.

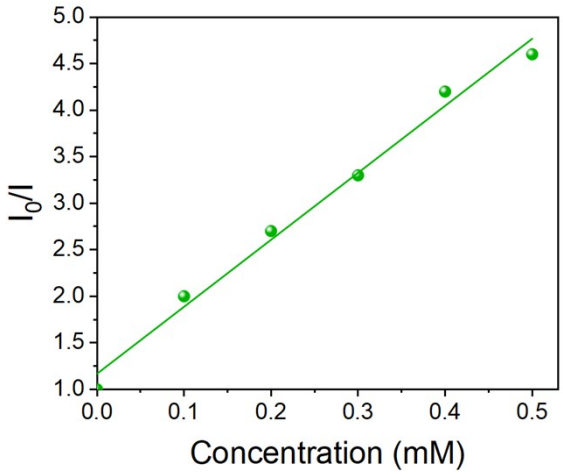

Figure S16. Stern Volmer plot of photoluminescence quenching of OAm/BVA-capped $CsPbBr_3$ NCs as a function of concentration of BTPA in DI water.

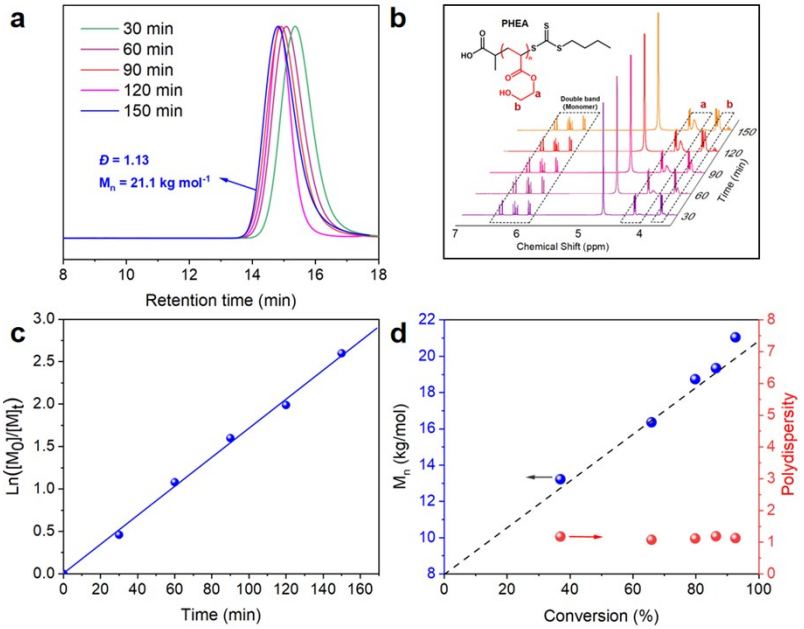

Figure S17. Kinetic study of photoinduced RAFT polymerization (monomer: HEA). (a) GPC curves, (b) ^{1}H NMR spectra (in $CDCl_3$, at 298 K, with 500 MHz), (c) plot of $Ln([M]_0/[M]_t)$ versus time and (d) theoretical molecular weight (dashed line), GPC molecular weight (blue), and polydispersity (red). Water-stable OAm/BVA-capped $CsPbBr_3$ NCs were used as photocatalysts in this polymerization.

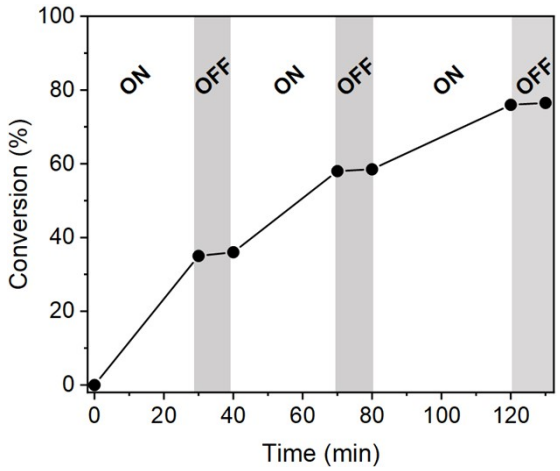

Figure S18 Light/dark cycling experiments for the photoinduced RAFT polymerization. Water-stable OAm/BVA-capped $CsPbBr_3$ NCs were used as photocatalysts in this polymerization.

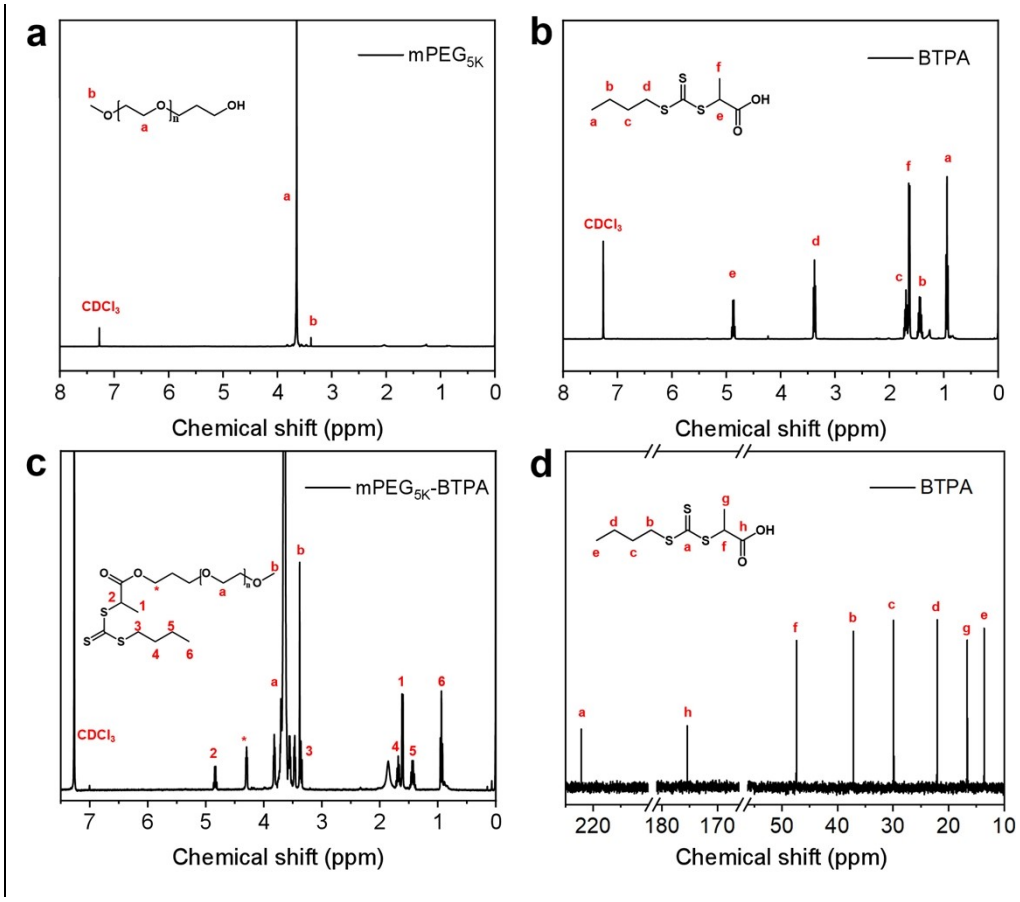

Figure S19. ^{1}H NMR spectra (in $CDCl_3$, at 298 K, with 500 MHz) of (a) monomethoxy poly (ethylene glycol) ($mPEG_{5K}$-OH), (b) 2-(butylsulfanyl)carbonothioyl sulfanyl propanoic acid (BTPA) RAFT agent, (c) $mPEG_{5K}$-BTPA macro-RAFT agent and (d) ^{13}C NMR spectra (in $CDCl_3$, at 298 K, with 500 MHz) of 2-(butylsulfanyl)carbonothioyl sulfanyl propanoic acid (BTPA) RAFT agent.

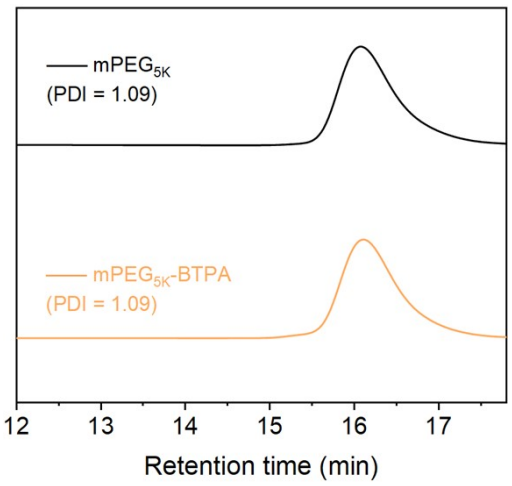

Figure S20. Gel permeation chromatography (GPC) curves of (a) $mPEG_{5K}$ and (b) $mPEG_{5K}$-BTPA macro-RAFT agent using dimethylformamide as eluent.

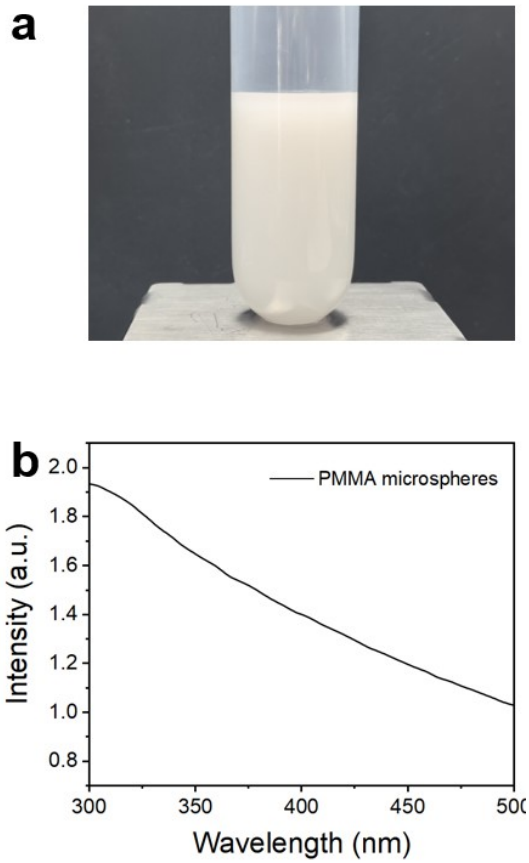

Figure S21. (a) Purified aqueous PMMA microsphere colloidal solution and (b) ultraviolet−visible absorption spectrum of PMMA microsphere prepared via $CsPbBr_3$-NC catalyzed photoinduced RAFT dispersion polymerization under blue light illumination (λ_{max} = 460 nm).

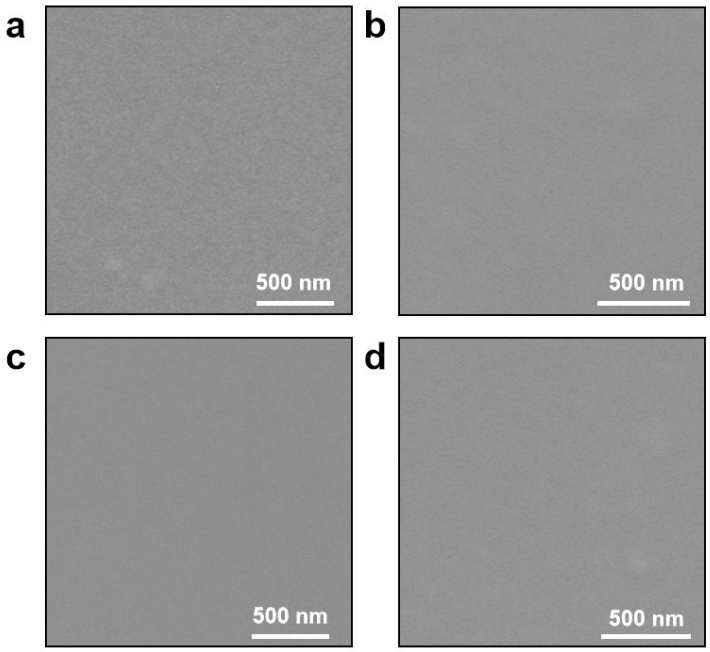

Figure S22. (a) The resulting product after polymerization of MMA without blue light irradiation with other reaction conditions fixed, (b) the resulting product after polymerization of MMA using conventional OAm/OA-capped $CsPbBr_3$ NC as photocatalyst with other reaction conditions fixed, (c) the resulting product after polymerization of MMA without RAFT agents with other reaction conditions fixed and (d) the resulting product after polymerization of MMA without deoxygenation process with other reaction conditions fixed.

Note: The SEM images show that there are almost no products and polymer microparticles after RAFT dispersion polymerization since the polymerization reaction did not proceed appropriately under these control conditions.

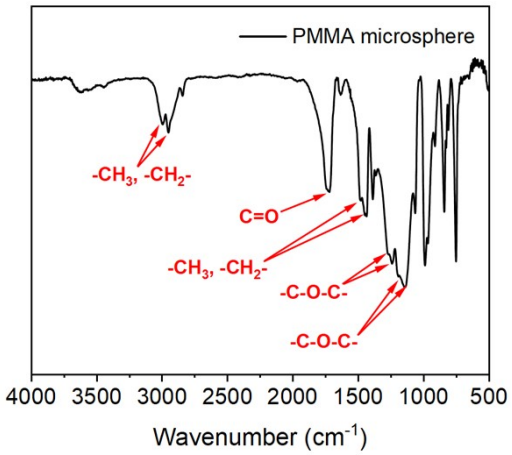

Figure S23. Fourier-transform infrared spectroscopy (FT-IR) of PMMA microsphere prepared via aqueous RAFT dispersion polymerization.

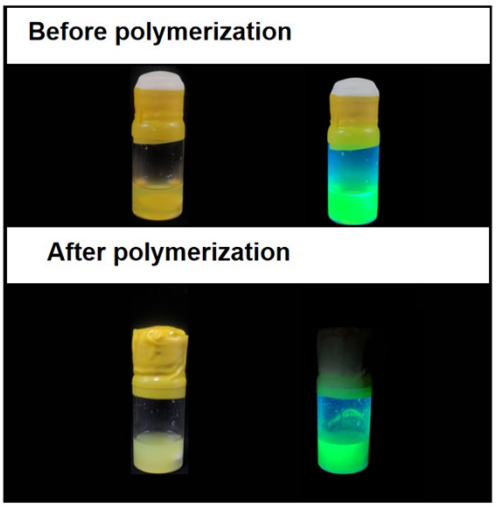

Figure S24 Digital photographs of the reaction system under ambient light and UV light before and after the dispersion polymerization.

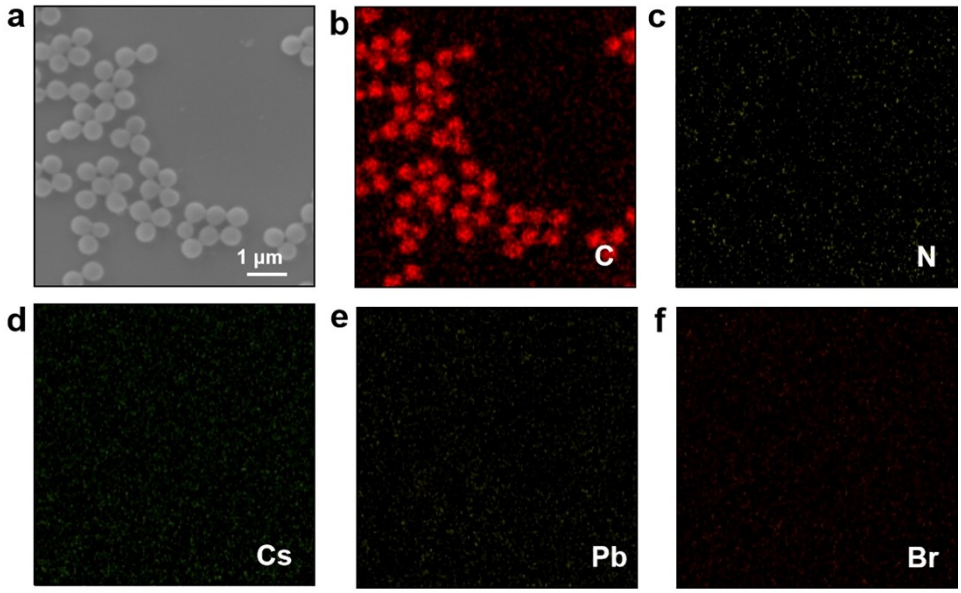

Figure S25. (a) Scanning electron microscope (SEM) image of PMMA microspheres, (b-f) elemental mapping analysis of PMMA microspheres. The ICP-MS indicates a residual lead content of only 0.32 wt%.

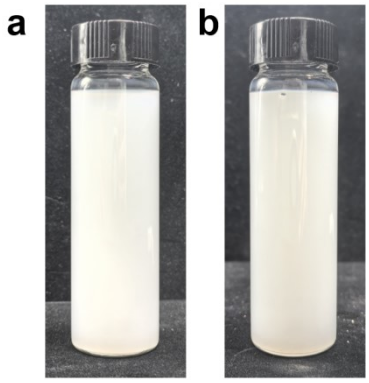

Figure S26. Long-term colloidal stability of the purified PMMA microspheres in the aqueous solution (a) right after RAFT dispersion polymerization and (b) after 30-day storage at ambient condition.

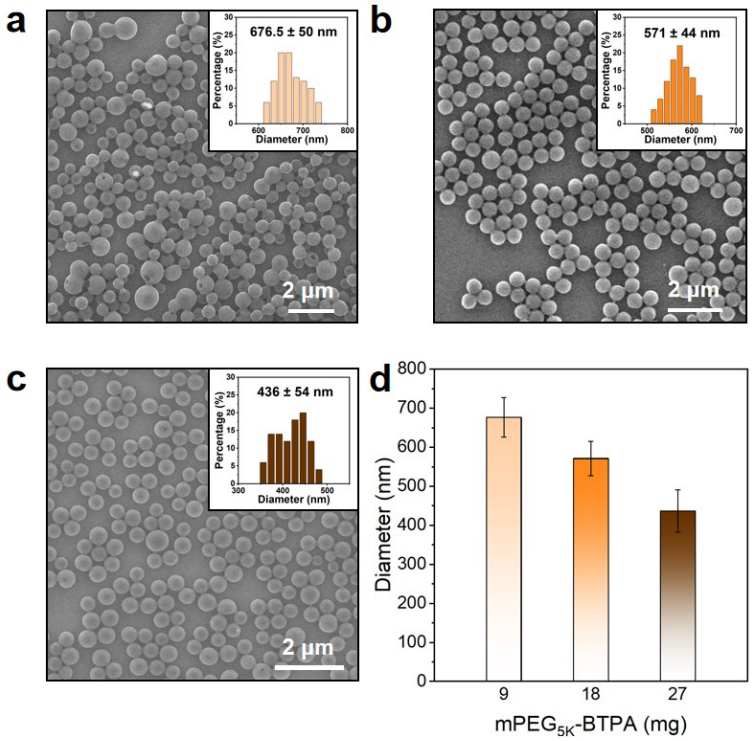

Figure S27. SEM images of PMMA microspheres prepared by photoinitiated RAFT dispersion polymerization of MMA with different quantities of $mPEG_{5K}$-BTPA: (a) 9 mg, (b) 18 mg and (c) 36 mg. Other polymerization conditions are identical to the typical synthesis protocol of PMMA microspheres shown in the previous experimental section. Water-stable OAm/BVA-capped $CsPbBr_3$ NCs were used as photocatalysts in this dispersion polymerization. (d) The statistical information of average microsphere diameter of PMMA microsphere shown in panels a to c.

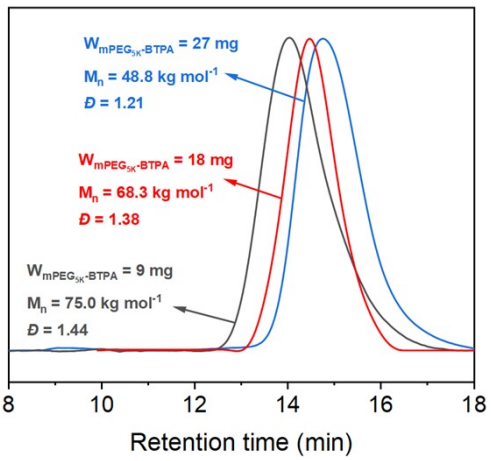

Figure S28. GPC curves of PMMA microspheres prepared by photoinitiated RAFT dispersion polymerization of MMA with different quantities of $mPEG_{5K}$-BTPA. Water-stable OAm/BVA-capped $CsPbBr_3$ NCs were used as photocatalysts in this dispersion polymerization.

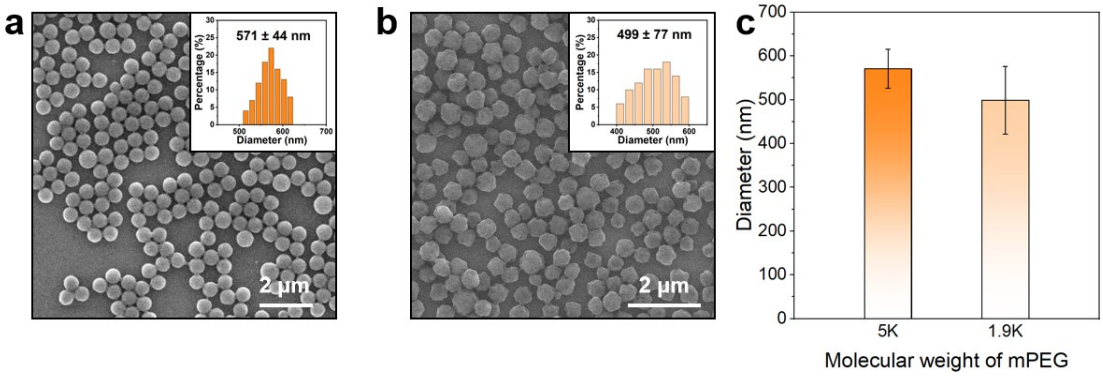

Figure S29. SEM images of PMMA microspheres prepared by photoinitiated RAFT dispersion polymerization of MMA employing 0.0034 mmol (a) $mPEG_{5K}$-BTPA and (b) $mPEG_{1.9K}$-BTPA as macro-RAFT agent, respectively. Other polymerization conditions are identical to the typical synthesis protocol of PMMA microspheres shown in the previous experimental section. Water-stable OAm/BVA-capped $CsPbBr_3$ NCs were used as photocatalysts in this dispersion polymerization. (c) The statistical information of the average microsphere diameter of the PMMA microsphere shown in panels a and b.

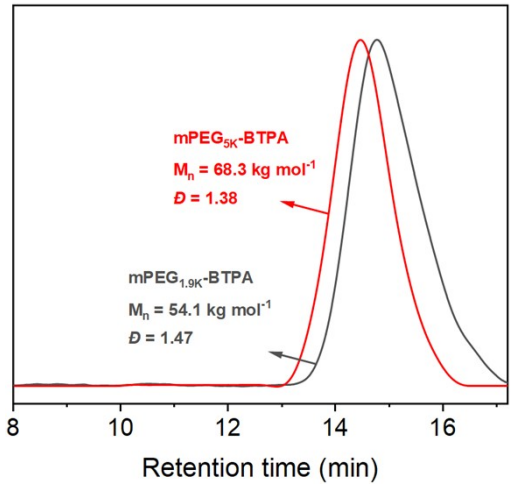

Figure S30. GPC curves of PMMA microspheres prepared by photoinitiated RAFT dispersion polymerization of MMA employing $mPEG_{5K}$-BTPA and $mPEG_{1.9K}$-BTPA as macro-RAFT agent. Water-stable OAm/BVA-capped $CsPbBr_3$ NCs were used as photocatalysts in this dispersion polymerization.

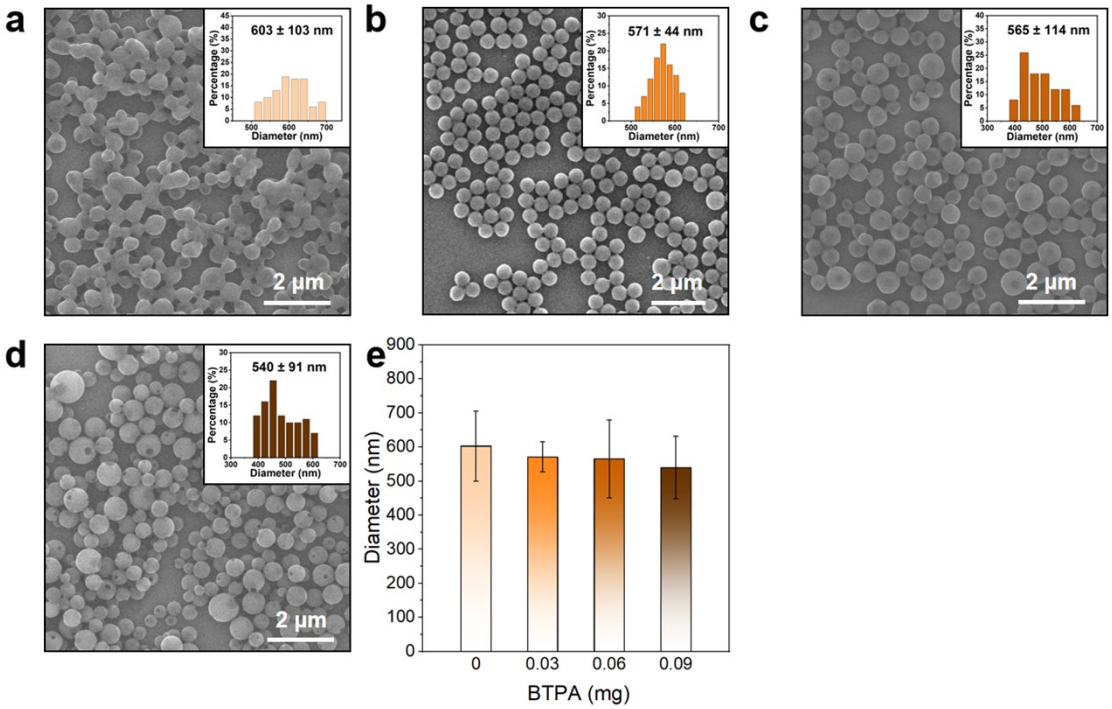

Figure S31. SEM images of PMMA microspheres prepared by photoinitiated RAFT dispersion polymerization of MMA with different quantities of BTPA: (a) 0 mg, (b) 0.03 mg, (c) 0.06 mg (d) 0.09 mg. Other polymerization conditions are identical to the typical synthesis protocol of PMMA microspheres shown in the previous experimental section. Water-stable OAm/BVA-capped $CsPbBr_3$ NCs were used as photocatalysts in this dispersion polymerization. (e) The statistical information of average microsphere diameter of PMMA microsphere shown in panels a to d.

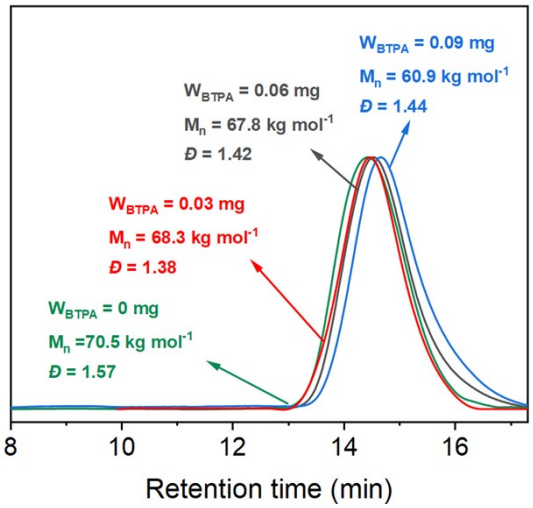

Figure S32. GPC curves of PMMA microspheres prepared by photoinitiated RAFT dispersion polymerization of MMA with different quantities of BTPA. Water-stable OAm/BVA-capped $CsPbBr_3$ NCs were used as photocatalysts in this dispersion polymerization.

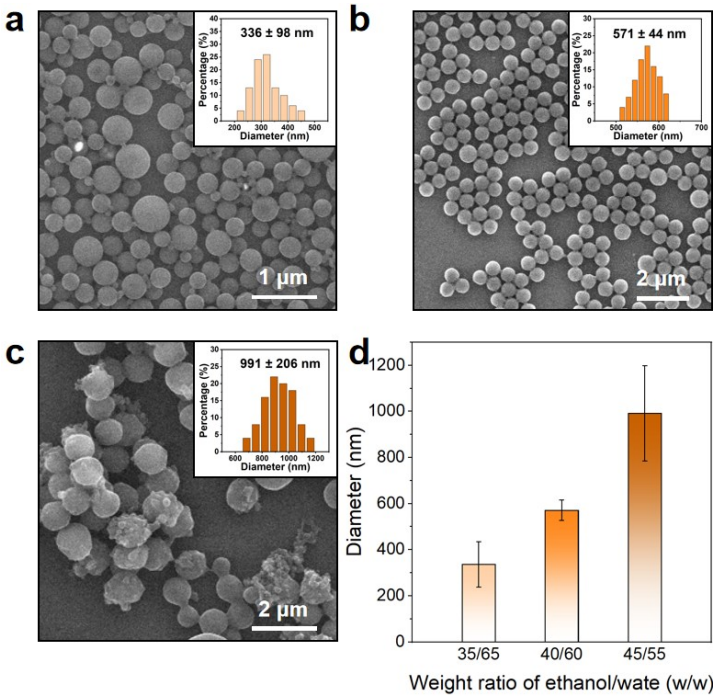

Figure S33. SEM images of PMMA microspheres obtained by photoinitiated RAFT dispersion polymerization of MMA with varied ethanol/water ratios (w/w): (a) 35/65, (b) 40/60, (c) 45/55. Other polymerization conditions are identical to the typical synthesis protocol of PMMA microspheres shown in the previous experimental section. Water-stable OAm/BVA-capped $CsPbBr_3$ NCs were used as photocatalysts in this dispersion polymerization. (d) The statistical information of the average microsphere diameter of PMMA microsphere shown in panel a to c.

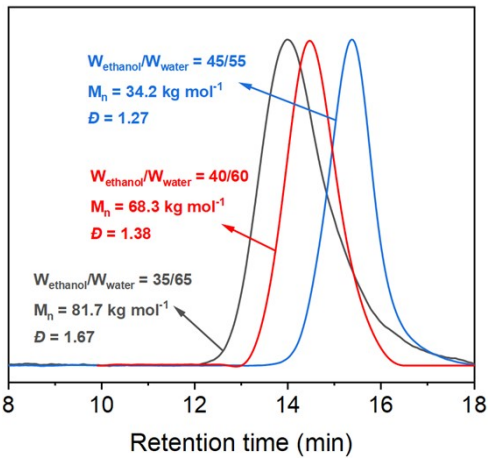

Figure S34. GPC curves of PMMA microspheres obtained by photoinitiated RAFT dispersion polymerization of MMA with varied ethanol/water ratios (w/w). Water-stable OAm/BVA-capped $CsPbBr_3$ NCs were used as photocatalysts in this dispersion polymerization.

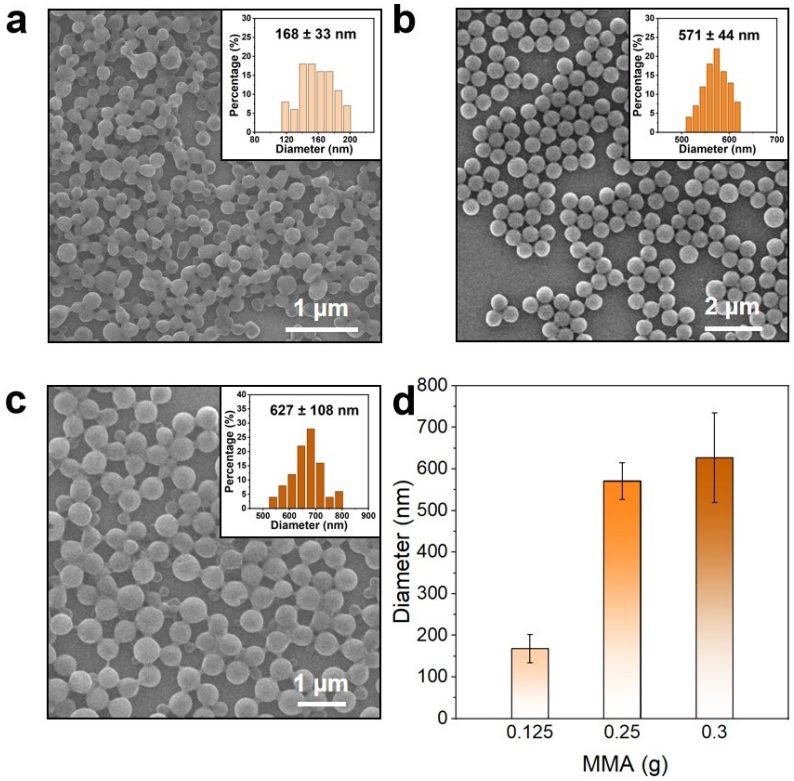

Figure S35. SEM images of PMMA microspheres prepared by photoinitiated RAFT dispersion polymerization with different quantities of MMA : (a) 0.125 g, (b) 0.25 g and (c) 0.3 g. Other polymerization conditions are identical to the typical synthesis protocol of PMMA microspheres shown in the previous experimental section. Water-stable OAm/BVA-capped $CsPbBr_3$ NCs were used as photocatalysts in this dispersion polymerization. (d) The statistical information of average microsphere diameter of PMMA microsphere shown in panels a to c.

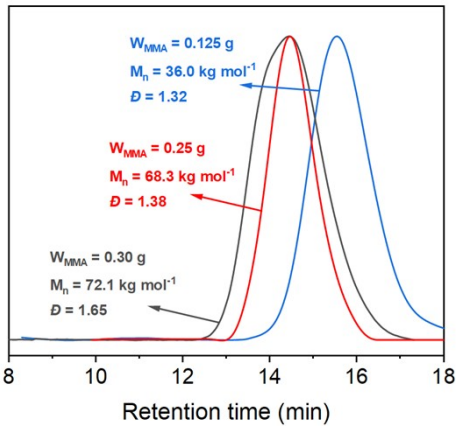

Figure S36. GPC curves of PMMA microspheres prepared by photoinitiated RAFT dispersion polymerization with different quantities of MMA. Water-stable OAm/BVA-capped $CsPbBr_3$ NCs were used as photocatalysts in this dispersion polymerization.

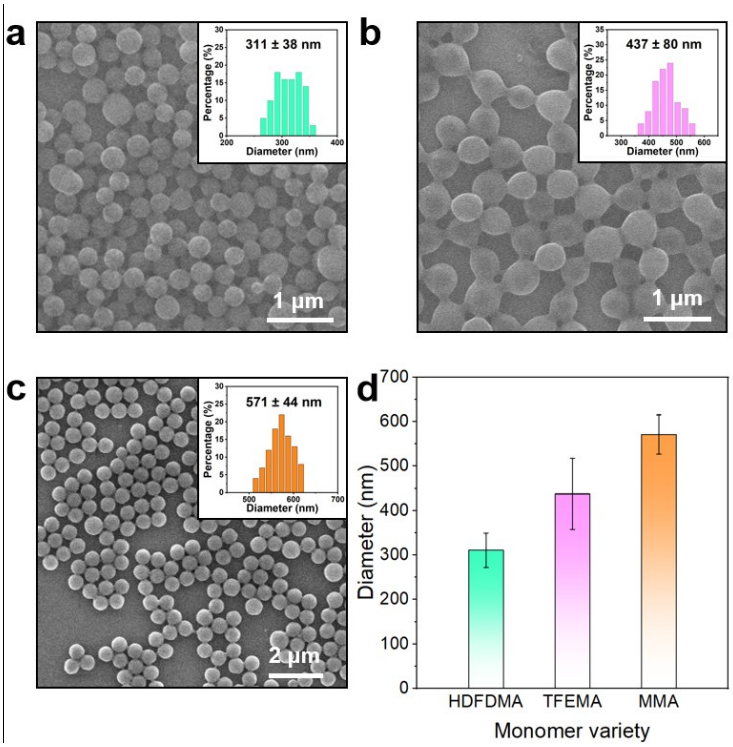

Figure S37. SEM images of polymeric microspheres prepared by photoinitiated RAFT dispersion polymerization with different vinyl monomers: (a) 3,3,4,4,5,5,6,6,7,7,8,8,9,9,10,10,10-heptadecafluorodecyl methacrylate (HDFDMA), (b) 2,2,2-trifluoroethyl methacrylate (TFEMA) and (c) PMMA. The polymerization conditions are identical to the typical synthesis protocol of PMMA microspheres shown in the previous experimental section except that the vinyl monomer was changed from MMA to HDFDMA and TFEMA. Water-stable OAm/BVA-capped $CsPbBr_3$ NCs were used as photocatalysts in this dispersion polymerization. (d) The statistical information of average microsphere diameter of PMMA microsphere shown in panels a to c.

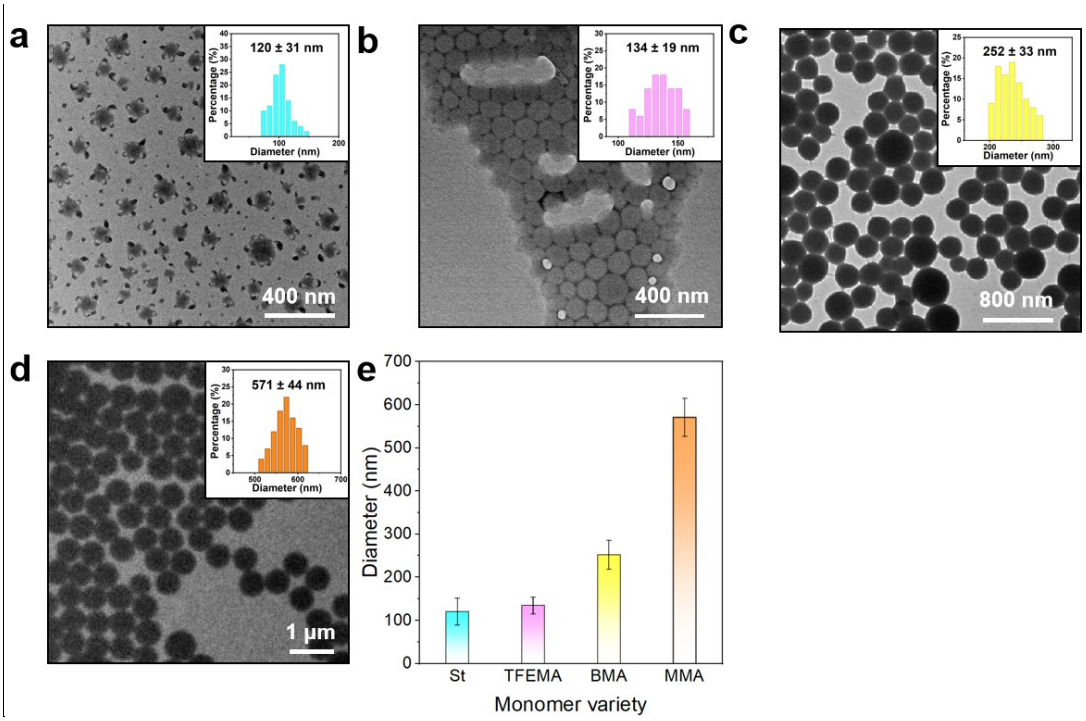

Figure S38. TEM images of polymeric microspheres prepared by photoinitiated RAFT dispersion polymerization with different monomer varieties: (a) styrene (St), (b) TFEMA, (c) butyl methacrylate (BMA) and (d) MMA. The polymerization conditions are identical to the typical synthesis protocol of PMMA microspheres shown in the previous experimental section except that the vinyl monomer is changed from MMA to St, TFEMA and BMA. Water-stable OAm/BVA-capped $CsPbBr_3$ NCs were used as photocatalysts in this dispersion polymerization. (e) The statistical information of average microsphere diameter of PMMA microsphere shown in panels a to d.

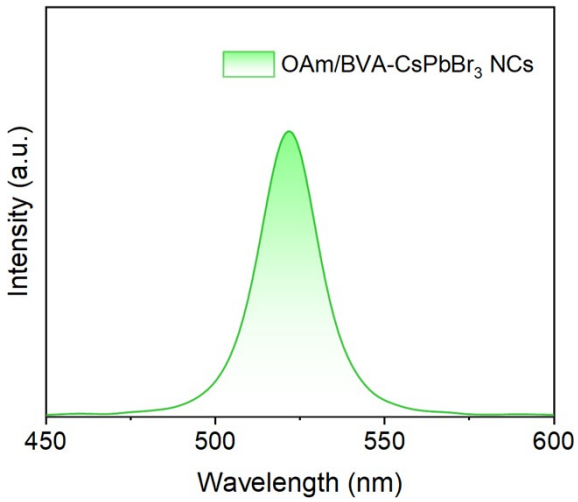

Figure S39. PL spectrum of OAm/BVA-capped $CsPbBr_3$ NCs dispersed in DI water under 808 nm near-infrared light irradiation.

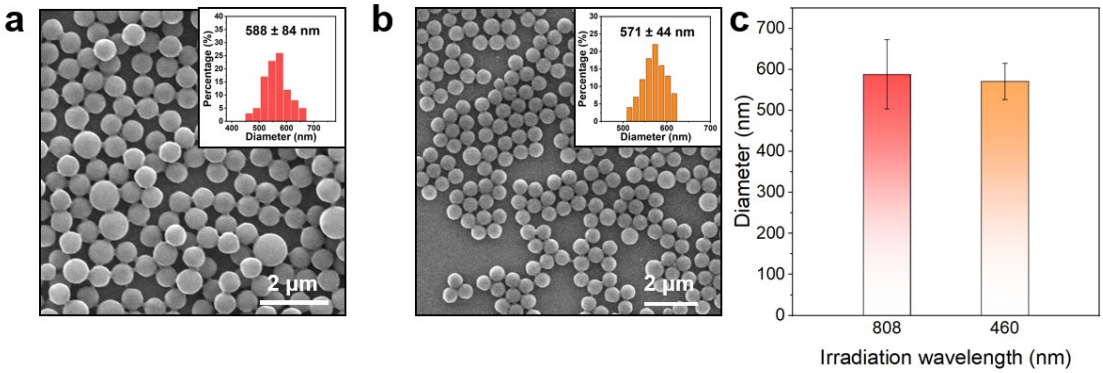

Figure S40. SEM images of PMMA microspheres prepared by photoinitiated RAFT dispersion polymerization of MMA with different irradiation wavelengths: (a) 808 nm, (b) 460 nm. Other conditions remained consistent with the primary synthesis protocol. Water-stable OAm/BVA-capped $CsPbBr_3$ NCs were used as photocatalysts in this dispersion polymerization. (c) The average diameters of PMMA microspheres shown in panels a and b.

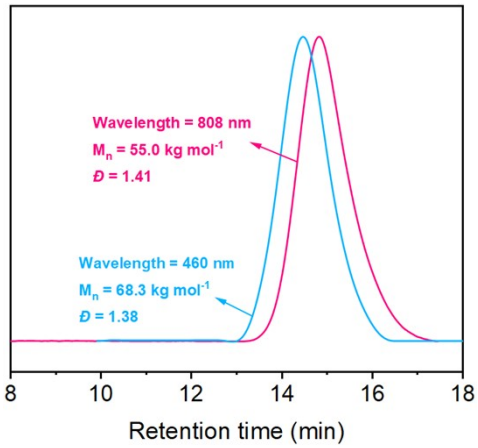

Figure S41. GPC curves of PMMA microspheres prepared by photoinitiated RAFT dispersion polymerization of MMA with different irradiation wavelengths. Water-stable OAm/BVA-capped $CsPbBr_3$ NCs were used as photocatalysts in this dispersion polymerization.

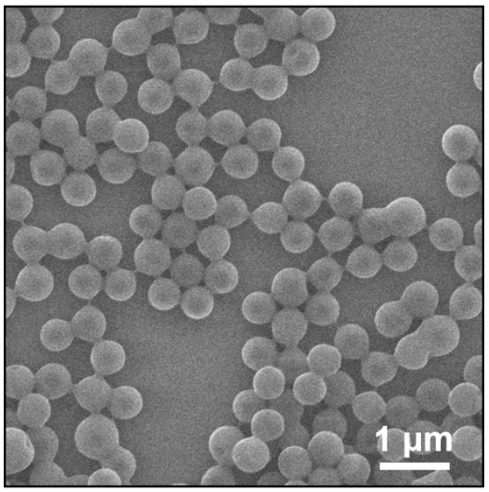

Figure S42. SEM image of PMMA microspheres prepared by photoinitiated RAFT dispersion polymerization of MMA under 808 nm irradiation. The polymerization solution is wrapped with paper during irradiation.

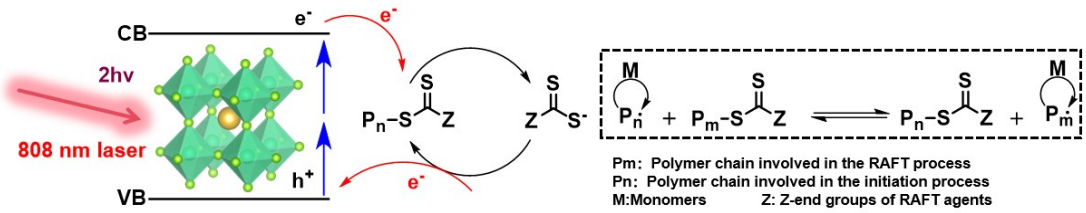

Figure S43. Near infrared light-induced RAFT dispersion polymerization of MMA catalyzed by OAm/BVA-capped $CsPbBr_3$ NCs via two-photon absorption mechanism.

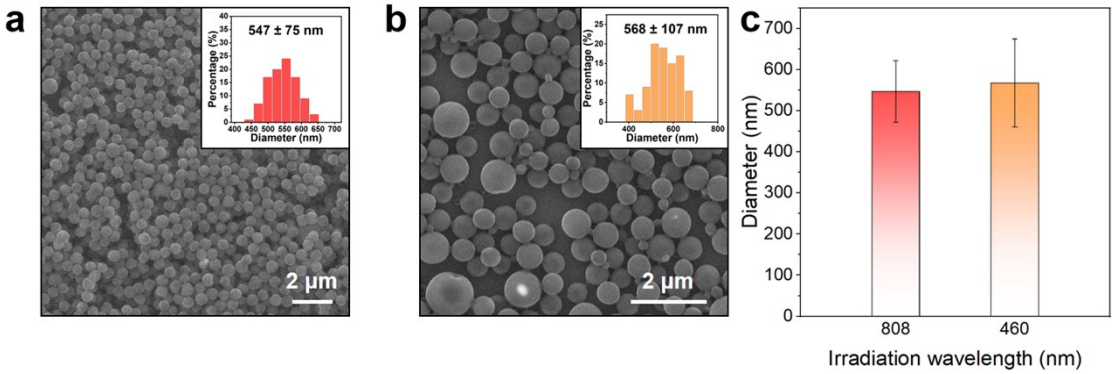

Figure S44. SEM images of large-scale (20× total reaction volume) preparation of PMMA microspheres prepared by photoinitiated RAFT dispersion polymerization of MMA with different irradiation wavelengths: (a) 808 nm, (b) 460 nm. Other conditions remained consistent with the primary synthesis protocol. Water-stable OAm/BVA-capped $CsPbBr_3$ NCs were used as photocatalysts in this dispersion polymerization. (c) The average diameters of PMMA microspheres shown in panels a and b. The reaction solution is irradiated under a near-infrared laser (λ_{max} = 808 nm and power = 100 mW/cm²) for 270 min.

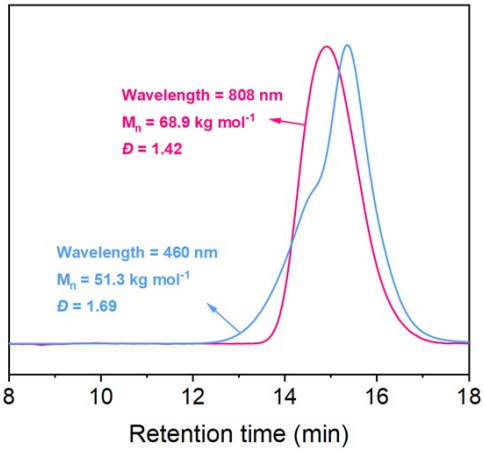

Figure S45. GPC curves of large-scale (20× total reaction volume) preparation of PMMA microspheres prepared by photoinitiated RAFT dispersion polymerization of MMA with different irradiation wavelengths. Water-stable OAm/BVA-capped CsPbBr3 NCs were used as photocatalysts in this dispersion polymerization.

References

1. Protesescu, L.; Yakunin, S.; Bodnarchuk, M. I.; Krieg, F.; Caputo, R.; Hendon, C. H.; Yang, R. X.; Walsh, A.; Kovalenko, M. V. Nanocrystals of Cesium Lead Halide Perovskites (CsPbX3, X = Cl, Br, and I): Novel Optoelectronic Materials Showing Bright Emission with Wide Color Gamut. *Nano Lett.* **2015**, *15* (6), 3692–3696.
2. Swift, T.; Swanson, L.; Geoghegan, M.; Rimmer, S. The pH-Responsive Behaviour of Poly(Acrylic Acid) in Aqueous Solution Is Dependent on Molar Mass. *Soft Matter* **2016**, *12* (9), 2542–2549.